EXAMINATION OF TWO DYNAMICALLY-DIFFERENT AREAS OF VERTICAL MOTION USING PC-GRIDDS

Matthew J. Bunkers

National Weather Service Office
Rapid City, South Dakota

Abstract

A case study of a modest early-winter cyclone is presented to illustrate the effectiveness of NOAA/NWS National Centers for Environmental Prediction (NCEP) model gridded data in identifying regions of upward vertical motion. Using the PC-Gridded Interactive Display and Diagnostic System (PC-GRIDDS) [a software program developed for manipulating model gridded data] and the 12-hour forecast from the nested-grid model (NGM), two distinct areas of upward vertical motion were identified. Each are concluded to have resulted from dynamically different processes. Although this is just one case study, the example illustrates some of the potential applications of gridded data to operational forecasting, and allows scientific reasoning to play an important role in the process.

1. Introduction

Gridded output data from the NOAA/NWS National Centers for Environmental Prediction (NCEP) numerical models have the potential to greatly enhance the operational methods of vertical motion estimation (Dunn 1991), as well as provide a better scientific understanding for the causes of sensible weather. As an example, the model vertical velocity can be compared to that estimated from quasi-geostrophic theory. This can be helpful for gaining an understanding of what might be responsible for producing the model vertical motion field, and can also be used to validate model performance. The PC-Gridded Interactive Display and Diagnostic System (PC-GRIDDS) is a software package capable of evaluating NCEP model gridded output data in significant detail and lends itself to the above objectives (Petersen 1992; Meier 1993). More recently, PC-GRIDDS has been shown to be effective in evaluating direct and indirect transverse ageostrophic jet-streak circulations (Labas 1994) and the coupling of jet-streaks to produce enhanced upward vertical motion (Noah 1994).

In this example, PC-GRIDDS is used to examine two separate areas of upward vertical motion attending a modest extratropical cyclone on 8 November 1994. The objective is to show how gridded data can be used to better understand the physical processes responsible for the formation of clouds and precipitation in a case where two dynamically-different processes were forcing the attendant vertical motion. One area of upward vertical motion was primarily associated with lower-tropospheric frontogenesis and a thermally-direct transverse ageostrophic circulation, while the second area was best represented by increasing cyclonic vorticity advection (CVA) with height. This case study is also intended to illustrate the plausibility of using PC-GRIDDS in a real-time situation to facilitate the operational forecasting process.

2. The Storm of Interest

During Tuesday, 8 November 1994, a 500-mb short-wave trough of weak to moderate amplitude was moving out of the south-central Rockies into the central plains of the United States (Fig. 1). This feature was associated with a large expanse of precipitation. By 0000 UTC 9 November, snow was falling over most of northeastern Colorado and the Nebraska panhandle (and also extended into southeastern South Dakota), well behind a surface cold front (Fig. 2a). At the same time, a band of rain extended along the frontal boundary from the Texas panhandle northeast into the southern Great Lakes region (Fig. 2a). Although a well-defined surface cyclone was not evident, a broad area of low pressure extended from northern Missouri to western Texas. Note the subtle break in precipitation from eastern Nebraska to southeastern Colorado separating the snow and rain. A dry slot in the visible satellite imagery (not shown) and warmer cloud top temperatures in the infrared satellite imagery were observed protruding into this region for nearly the same time (Fig. 2b). Of additional interest, the northern edge of the snow was very near the center of a surface anticyclone, similar to a case presented by Hakim and Uccellini (1992).

The upper-level flow was divided into two "branches" over the Pacific Northwest, and joined together again over the northern Great Lakes (Fig. 3a). The short-wave trough mentioned earlier is clearly identifiable in the observed wind field that existed at 300 mb across Wyoming, Colorado, and western New Mexico (Fig. 3b). Since the weather system of interest was moving into an increasingly confluent flow aloft (and assuming that no further jet maxima were going to traverse the base of the trough), one would expect a general weakening of the storm system with time. The southern branch of the polar jet stream was noted in proximity to both the snow and rain areas, and eventually merged with the northern branch over the Great Lakes (Figs. 3a-b).

Two jet-streaks can be identified across the area of concern: (1) the first (and weaker) one was noted in proximity to the base of the upper-level trough in New Mexico (~ 110 knots), and (2) the second one extended east across Minnesota and the Great Lakes (~ 130 knots) (Fig. 3a-b). The area of precipitation in northeastern Colorado and the Nebraska panhandle was relatively near the left exit region of the first (cyclonically-curved) jet, and the precipitation along the front was in proximity to the right entrance region of the second (anticyclonically curved) jet. The two jets did not appear to be acting in tandem (i.e., they were not coupled as in Uccellini and Kocin 1987). In general, entrance and exit regions of jet-streaks have been widely associated with transverse ageostrophic circulations favorable for upward vertical motion as revealed by observational (Uccellini 1990; Labas 1994) and modeling studies (Moore and VanKnowe 1992).

Additionally, the effects of jet-streak curvature have implications for the observed precipitation pattern. Using a simple two-layer primitive equation model, Moore and VanKnowe (1992) found that primarily a two-cell pattern of vertical motion

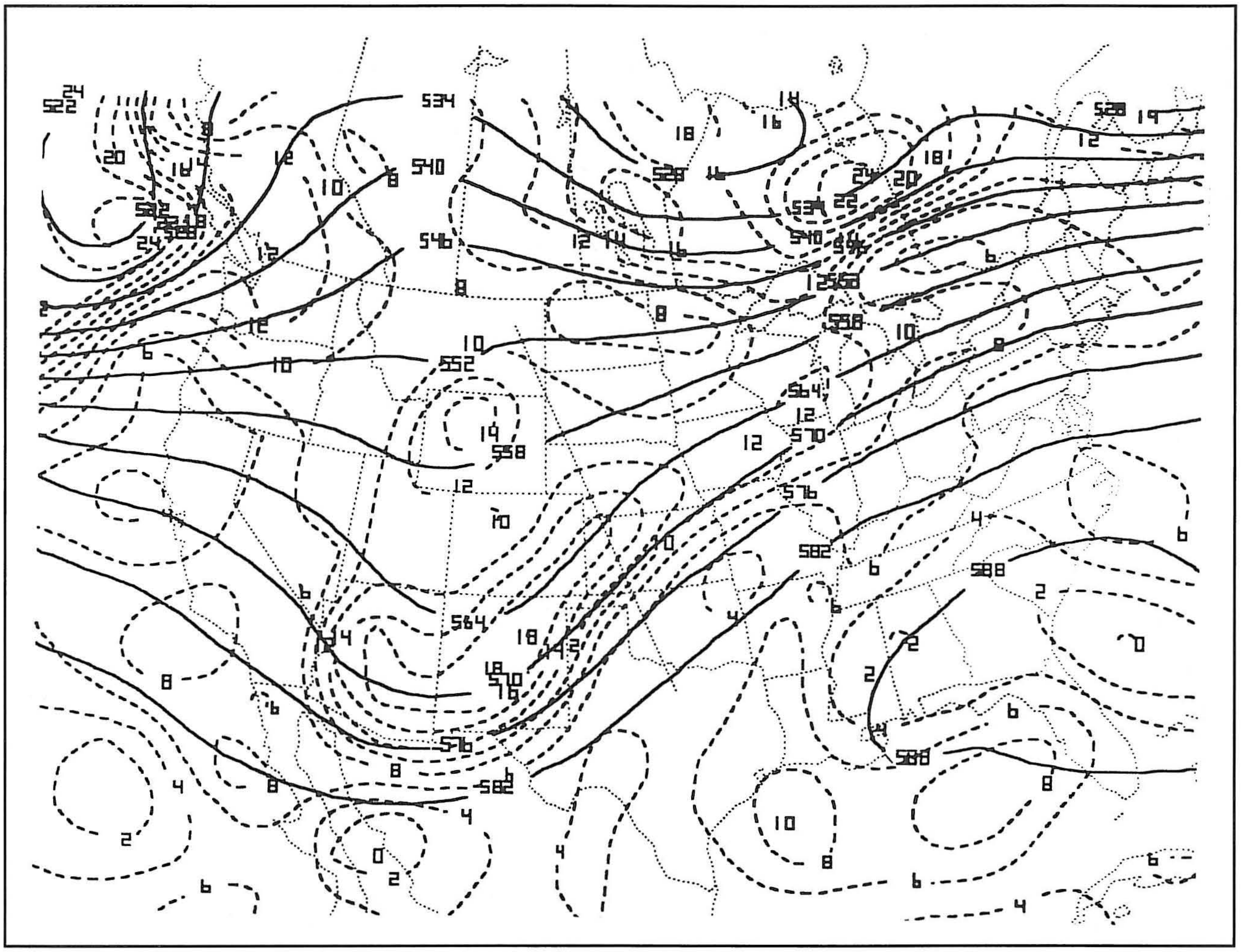

Fig. 1. The 00-hour NGM analysis of the 500-mb heights (solid, 6 dm intervals) and vorticity (dashed, $2 \times 10^{-5}\ s^{-1}$ intervals) valid 0000 UTC 9 November 1994. The thin dotted line from Montana to Texas represents the cross-section used in related figures (48° N, 106° W to 33° N, 98° W).

was concomitant with cyclonically and anticyclonically curved jet-streaks rather than the four-cell pattern commonly associated with straight jets. Also, the vertical-motion centers for the curved jets were stronger than for a straight jet and aligned nearer to the jet axis as opposed to across it. For the cyclonically-curved jet, the upward vertical motion was strongest near and to the left of the jet axis in the exit region, while the strongest upward vertical motion was observed near and to the right of the jet axis in the entrance region for the anticyclonically-curved jet. This modeled pattern of ascent appears to be reflected by the two slightly curved jet-streaks and the related precipitation pattern of this case (Figs. 2a and 3a)

A cross-section (perpendicular to the 850-300 mb thickness field, and thus in general to the surface front) of equivalent potential temperature (Θ_e) and wind speeds from Glasgow, Montana (GGW) to Dallas, Texas (FWD) reveals the structure that was associated with the low-level front (Fig. 4). The Θ_e contours (dashed) were tightly packed in the frontal zone, which intersected the surface between Dodge City, Kansas (DDC) and Norman, Oklahoma (OUN). The front was rather shallow as it extended well to the north before it became ill-defined above GGW. The Θ_e gradient also relaxed somewhat near Rapid City, South Dakota (RAP), where the precipitation abruptly ended (Fig. 2a). The frontal zone exhibited a large horizontal temperature gradient and large static stability, as can be inferred from the strong Θ_e gradient. The above observations are consistent with the structure that has been observed with many surface fronts (Keyser 1986).

The strong jet core of $> 55\ m\ s^{-1}$, observed above North Platte, Nebraska (LBF) and DDC (Fig. 4), is consistent with Fig. 3a. No other jets are observed. Note how the Θ_e isopleths fanned out to the south of the jet core, with the tropopause being lower on the north side of the jet relative to the southern side of the jet. [The position of the tropopause can be inferred by locating the boundary of large static stability in the upper troposphere.] This is a classic feature of well-developed upper-level jets and follows from the thermal wind relationship (Holton 1992). An area of relatively tightly packed Θ_e contours also protruded downward on the underside of the jet core to the south, which is indicative of an upper-level front and potential tropopause fold (Keyser 1986; Shapiro and Keyser 1990). Based on these limited analyses, it appears that the precipitation may have been caused by a combination of frontal forcing (either upper- or lower-tropospheric) and transverse jet-streak circulations (which can lead to tropopause folding); yet it is difficult to discern the specific dynamical cause(s) of upward vertical

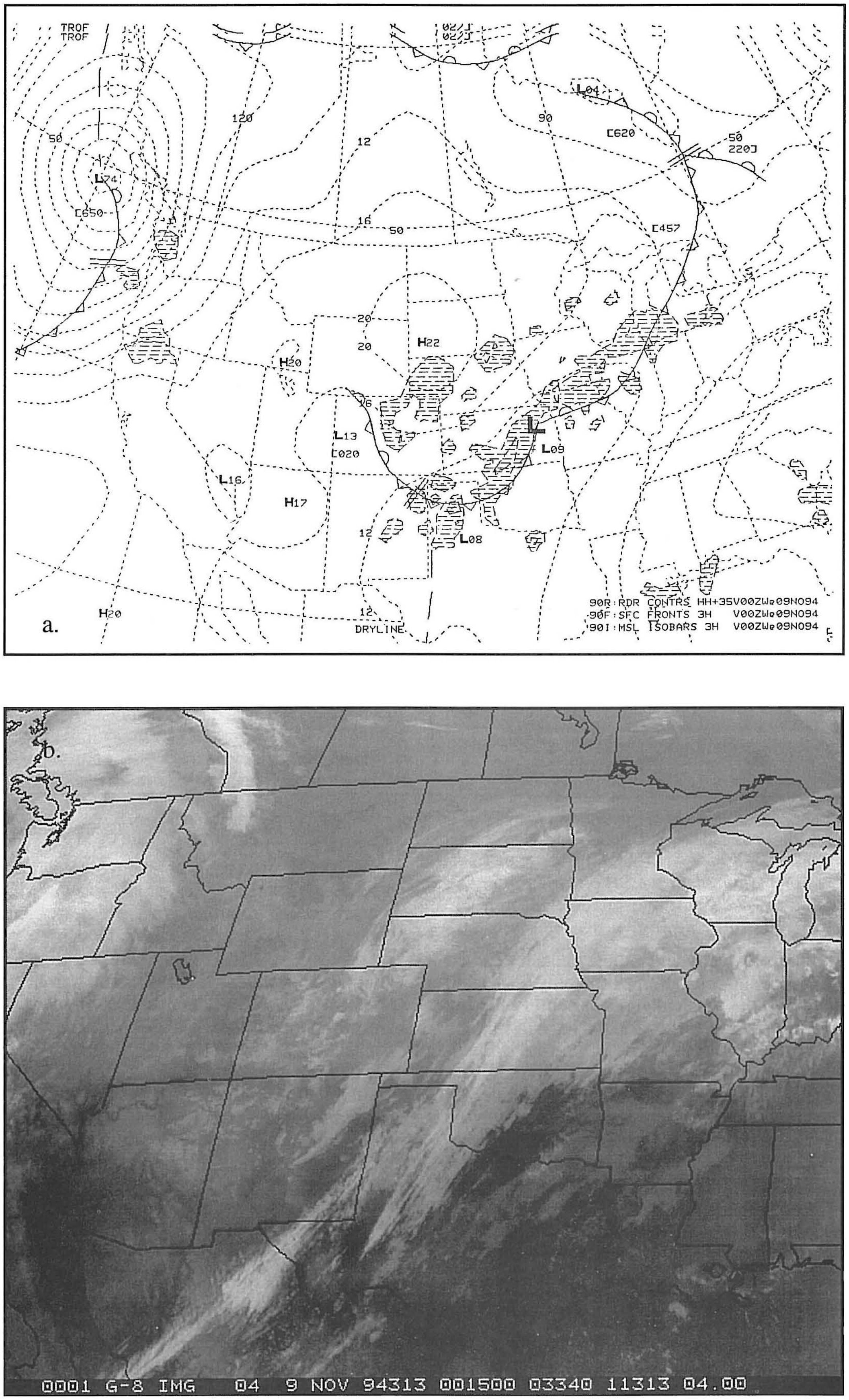

Fig. 2. (a) NWS Automation of Field Operations and Services (AFOS) composite of the NCEP-derived surface fronts and sea-level isobars (dashed, 4 mb intervals) valid 0000 UTC 9 November 1994, and radar echoes valid 0035 UTC 9 November 1994. (b) Infrared satellite image valid 0015 UTC 9 November 1994.

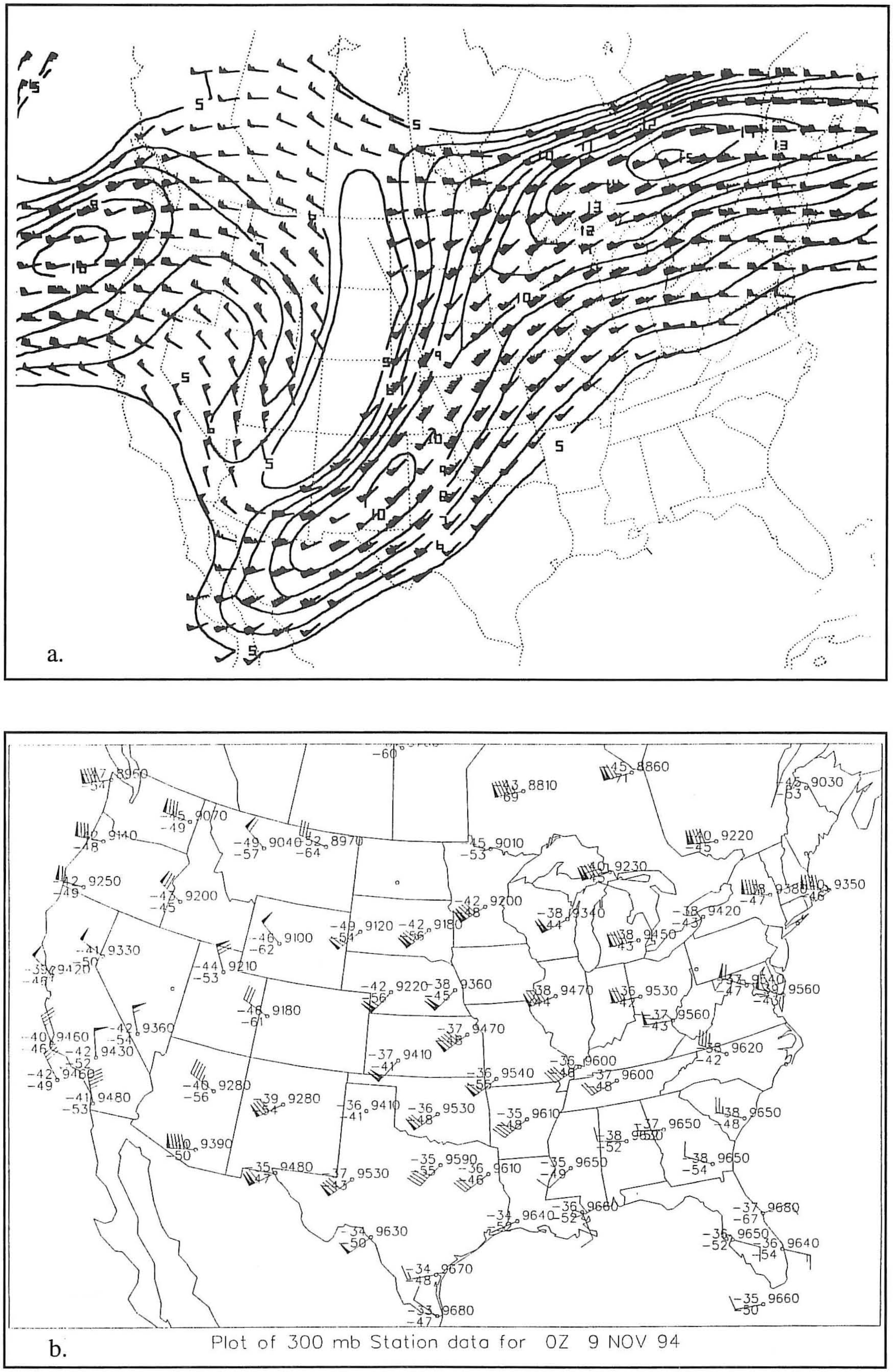

Fig. 3. (a) The 00-hour NGM analysis of the 300-mb wind speeds (solid, 1×10^1 knot intervals, ≥ 50 kt), and wind barbs (≥ 50 kt) valid 0000 UTC 9 November 1994. The thin dotted line is the same as in Fig. 1. (b) WXP (Purdue Weather Processor via Unidata) conventional 300-mb station plots valid 0000 UTC 9 November 1994.

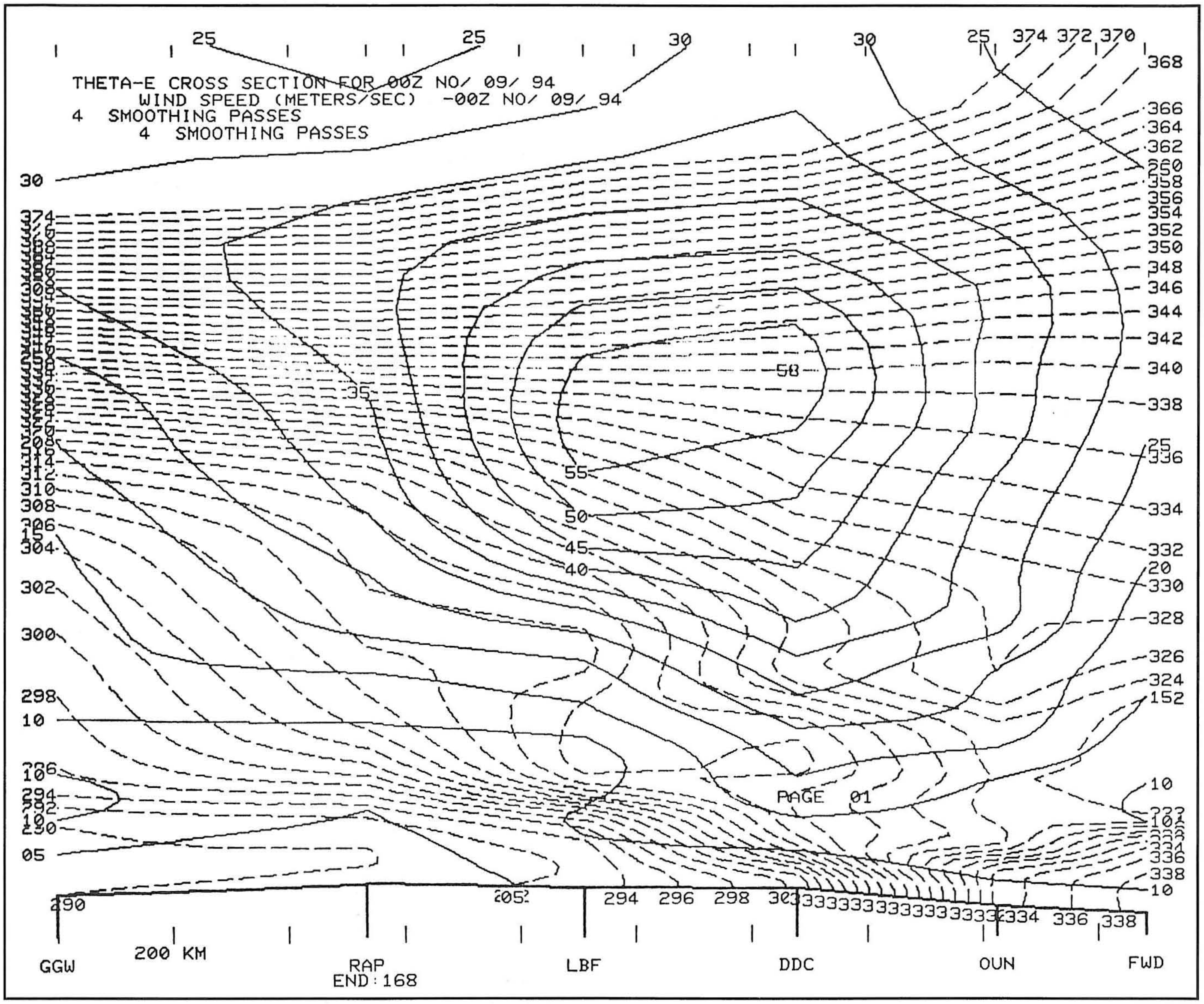

Fig. 4. NWS Automation of Field Operations and Services (AFOS) cross-section plot of wind speeds (solid, 5 m s^{-1} intervals) and equivalent potential temperature (dashed, 2 K intervals) from Glasgow, Montana to Dallas, Texas valid 0000 UTC 9 November 1994.

motion for the respective precipitation bands based on these data alone. In addition, from an operational perspective it would be beneficial to anticipate these conditions well in advance, rather than to rely on an analysis. Therefore, PC-GRIDDS and the 12-hour forecast of the nested-grid model (NGM) will be used to: (a) determine if the above analyses were correctly forecast, and (b) examine the exact nature of the upward vertical motion attending both precipitation bands.

3. Evaluation using PC-GRIDDS

a. Verification of the forecast

The following discussion utilizes the gridded data from the 12-hour forecast of the NGM, initialized at 1200 UTC 8 November 1994. The horizontal resolution of the NGM is 83 km at 45 °N and it has 16 layers. However, only the mandatory levels are available for PC-GRIDDS, effectively reducing the vertical resolution to 9 layers. This model appeared to provide a realistic representation of the atmospheric processes, and was initialized adequately well. A cross-section (48° N, 106° W to 33° N, 98° W) was constructed to coincide as closely as possible with that of Fig. 4 for a qualitative comparison.

The NGM provided a reasonable forecast of the 300-mb wind speed and split flow pattern; however, the model failed to accurately depict the second jet maximum over New Mexico and far western Texas at only 12 hours into the forecast cycle (Fig. 5). [Albeit, this second jet was slightly better forecast at the 200 and 400-mb levels.] The 130+ knot jet-streak over the Great Lakes region was in very good agreement between the model forecast and upper-air observations (Figs. 3a-b and 5). In contrast, wind speeds of only 90 knots were forecast in southern New Mexico (Fig. 5) where observations indicated 110 knots (Fig. 3b). The "underforecast" jet-streak was likely in part a result of the data paucity over Mexico, and this ten-

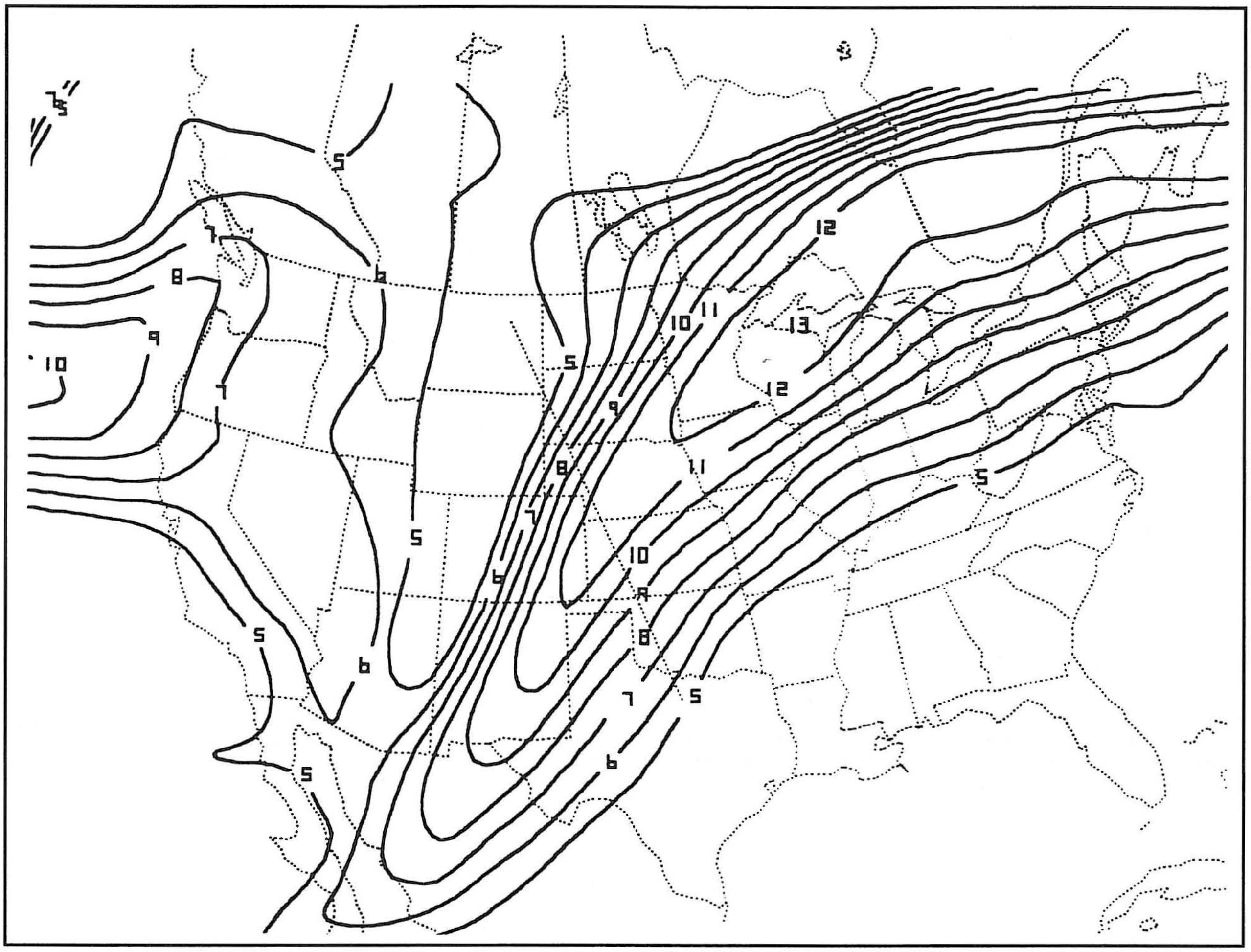

Fig. 5. The 12-hour NGM forecast of the 300-mb wind speeds (solid, 1×10^1 knot intervals, ≥ 50 kt) valid 0000 UTC 9 November 1994. The thin dotted line is the same as in Fig. 1.

dency of underprediction of jet-streak strength by the NGM has been noted previously (Barnes and Colman 1994).

Further application of PC-GRIDDS illustrates that the 12-hour forecast of the NGM successfully depicted the *general* location and intensity of the low-level front when compared to the analyzed cross-section (Figs. 4 and 6). Low-level packing of the potential temperature (Θ) contours was noted from near 36° N to 47° N, where the front became less recognizable above GGW (Fig. 6). As mentioned earlier, surface-based frontal zones are characterized by large static stability and horizontal temperature gradients, which are manifested in relatively large potential temperature (or Θ_e) gradients within the frontal zone. This type of pattern is consistent between Figs. 4 and 6, and indicates a reasonable prediction by the NGM. [Note that although a comparison is made between Θ and Θ_e, both parameters tend to be concentrated in frontal zones, thus a *general* comparison can be made.] The wind speed and pattern are also in agreement between the model and observations, with only a slightly stronger jet depicted by the NGM. Additional confirmation of the surface frontal position is gained by viewing a cross-section of the normal component of the geostrophic wind (not shown), where post-frontal northeasterly flow corresponds to negative values (i.e., flow out of the cross-section).

Although the vertical resolution of PC-GRIDDS is rather course (i.e., only the mandatory levels), the 12-hour forecast of the NGM indicated an upper-level front just below the jet stream and supports the existence of the tropopause fold mentioned earlier (Fig. 7a). In Fig. 7a, the tropopause is delineated by the 1×10^{-5} K mb^{-1} s^{-1} potential vorticity contour (consistent with other studies), separating high static-stability stratospheric air above from lower static-stability tropospheric air below. The potential vorticity-delineated stratospheric protrusion coincides with the relatively stronger potential temperature gradient observed descending toward 400 mb (Fig. 7a). The upper-level front and tropopause fold are also a region of pronounced cyclonic vorticity and horizontal and vertical wind shear (Figs. 6 and 7b). Note the extrusion of high cyclonic vorticity air from near 250 mb down through 400 mb (Fig. 7b), and the strong wind shear (gradient) in the same region (Fig. 6), which are again consistent with the pattern in Fig. 7a (Keyser 1986). In general, this forecast agrees well with the observed tropopause and upper-level front depicted in Fig. 4. A cross-section of absolute momentum (not shown) further substantiates the existence and location of the upper-tropospheric front, as it has been shown to be an appropriate frontal defining parameter (Shapiro 1981). Figures 6 and 7a-b demonstrate that using PC-GRIDDS to analyze gridded model output can be an effective method for implying the existence of certain mesoscale features (e.g., upper-level fronts) that operational meteorologists were previously unable to discern using conventional methods.

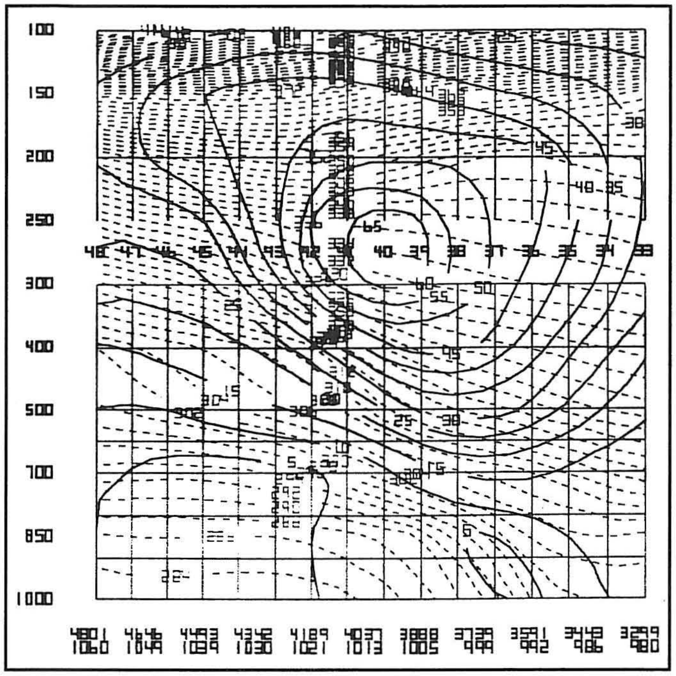

Fig. 6. The 12-hour NGM forecast cross-section of the wind speeds (solid, 5 m s^{-1} intervals) and potential temperature (dashed, 2 K intervals) from 48 °N, 106 °W to 33 °N, 98 °W valid 0000 UTC 9 November 1994. Vertical lines are latitude (°N) and horizontal lines are pressure (mb). The first row of numbers along the abscissa is latitude (1 × 10^2 °N) and the bottom row of numbers is longitude (1 × 10^1 °W).

The pattern of upper-level frontogenesis was quantified by using a formulation of the Petterssen frontogenesis function, as derived by Keyser et al. (1988). Neglecting diabatic and tilting effects, the scalar frontogenesis function is ($F_n < 0$ denotes frontogenesis):

$$F_n = -\frac{d}{dt}\,|\nabla\Theta| = -\frac{1}{|\nabla\Theta|}(\vec{\psi}\cdot\nabla\Theta), \qquad (1)$$

where Θ is the potential temperature, ∇ is the two-dimensional gradient operator, and:

$$\vec{\psi} = \left(-\frac{\partial u\partial\Theta}{\partial x\,\partial x} - \frac{\partial v\partial\Theta}{\partial x\,\partial y}\hat{i}, \; -\frac{\partial u\partial\Theta}{\partial y\,\partial x} - \frac{\partial v\partial\Theta}{\partial y\,\partial y}\hat{j}\right) \qquad (2)$$

is a Cartesian formulation of the two-dimensional F-vector described by Keyser et al. (1988). Equation (1) represents an expression for the individual rate of change of the magnitude of the horizontal potential temperature gradient. The component of the Keyser et al. (1988) F-vector normal to the potential temperature isopleths is the frontogenetic component (F_n or ψ_n). Note that if the geostrophic wind is used in place of the actual wind in (2), and each component is multiplied by R/p, this becomes the more familiar Q-vector. Referring to Fig. 7a, it is inferred that upper-level frontogenesis was occurring near the 400-mb level. The scalar frontogenesis function applied at this level does indeed indicate frontogenesis between roughly 44° N and 40° N (Fig. 8), which is consistent with Fig. 7a. Also note that this upper-tropospheric frontogenesis was maximized on the poleward side of the 300-mb jet stream (compare with Fig. 5).

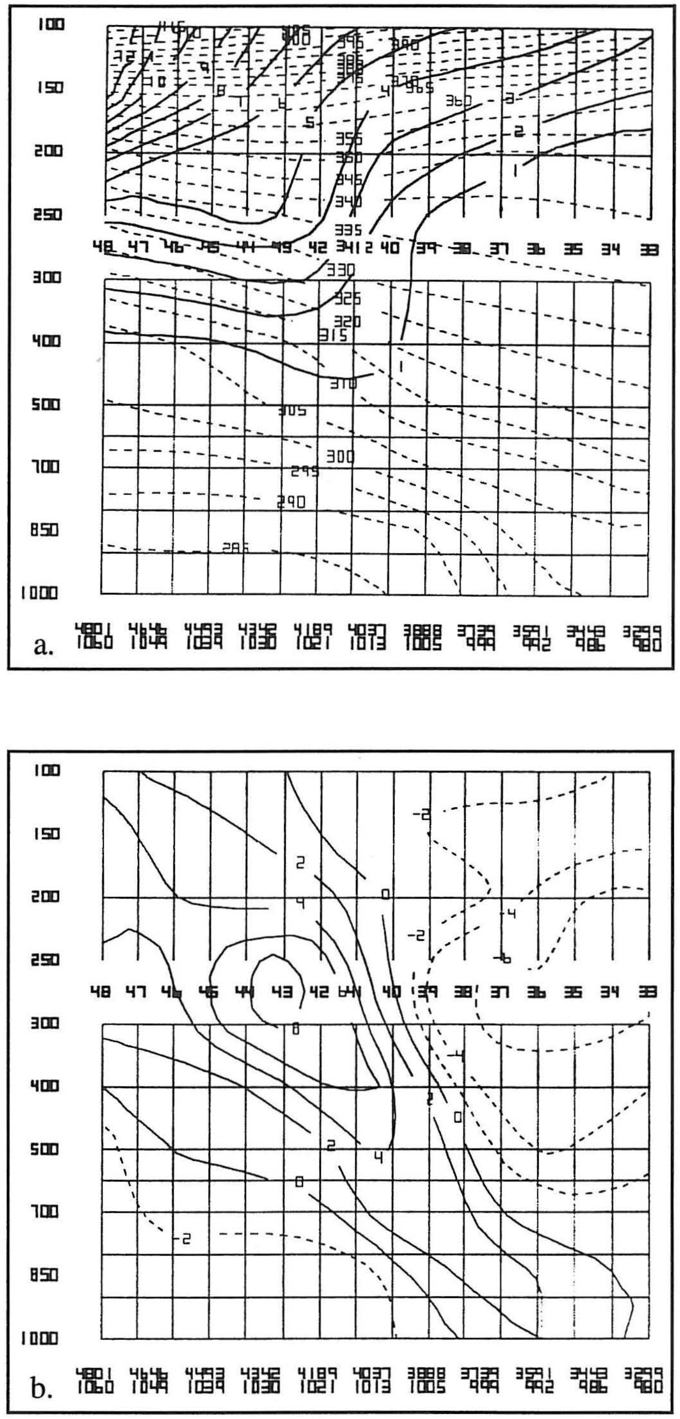

Fig. 7. The 12-hour NGM forecast cross-section of: (a) potential vorticity (solid, 1 × 10^{-5} K mb^{-1} s^{-1} intervals) and potential temperature (dashed, 5 K intervals), and (b) relative vorticity (dashed negative, 2 × 10^{-5} s^{-1} intervals) valid 0000 UTC 9 November 1994. Cross-section same as Fig. 6.

b. Evaluation of vertical motion

The 12-hour NGM forecast of vertical velocity indicated two distinct areas of upward vertical motion across the central United States (Figs. 9a-b). The strongest vertical motion along the cross-section (−6 μbar s^{-1}), between 37° N and 33° N, was associated with the rain in Oklahoma and Texas which

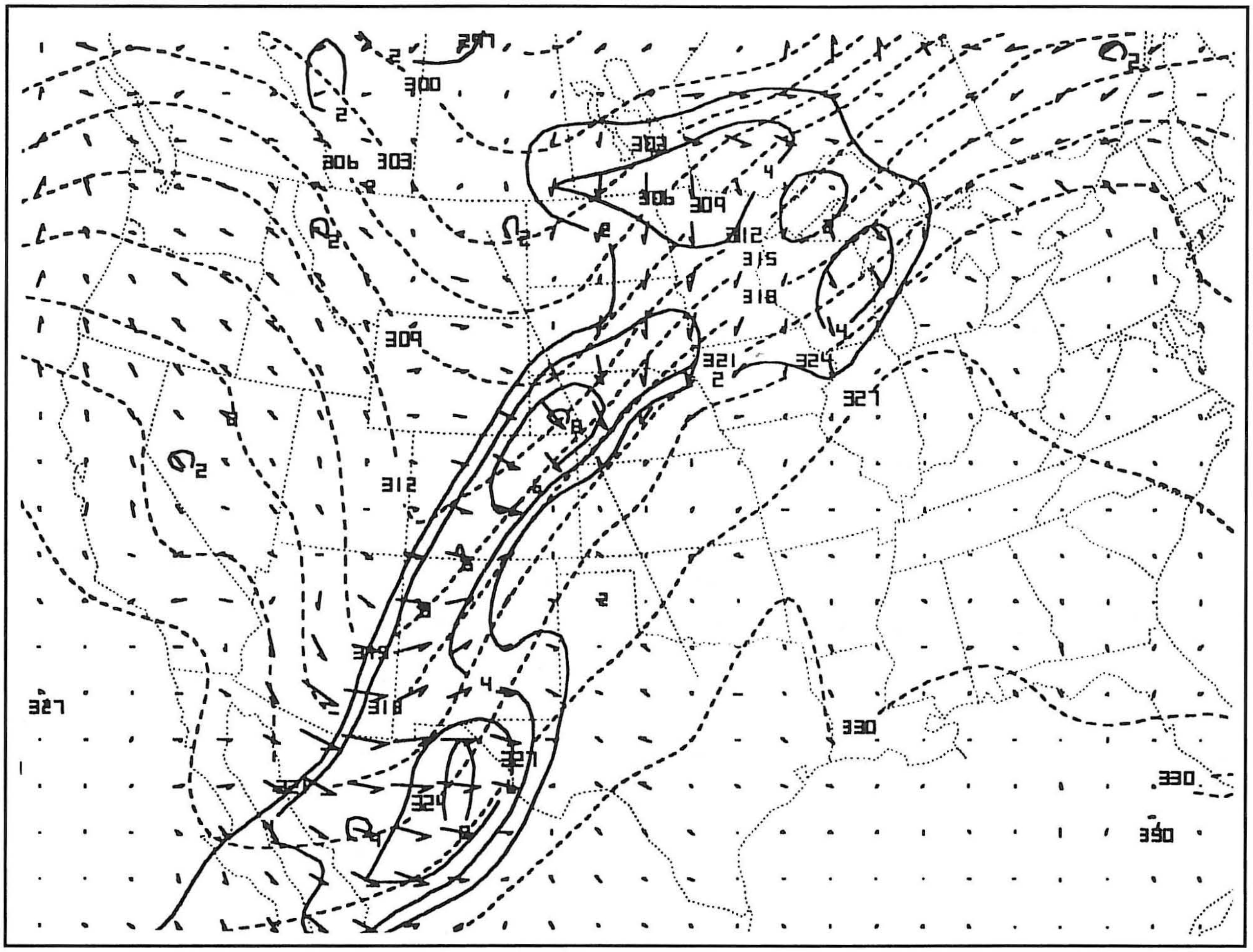

Fig. 8. The 12-hour NGM forecast of the: 400-mb scalar frontogenesis function (solid positive, 2×10^{-10} K m^{-1} s^{-1} intervals), potential temperature (dashed, 3 K intervals), and ψ-vectors valid 0000 UTC 9 November 1994. The frontogenesis function was multiplied by negative one so that positive values denote frontogenesis. The thin dotted line is the same as in Fig. 1.

was occurring along the surface frontal zone (Fig. 9a). The second maximum (-3 μbar s^{-1}), located between 43° and 40° north, was associated with the snow band in Colorado and Nebraska (which was closer to the surface high pressure center than the surface front). Note that the "traditional" 700-mb vertical velocity display (Fig. 9b) does not show as strong of an upward vertical motion for this second case, which might have misled the forecaster. Additionally, although the general pattern of vertical motion is consistent with the precipitation pattern, the upward vertical motion pattern is displaced slightly to the south of the precipitation (Figs. 2a-b and 9b). The possibility that the area of downward vertical motion (Figs. 9a-b) juxtaposed with the area of strong upward motion could signal the presence of an ageostrophic transverse circulation will be examined below. This vertical motion profile helps to explain the subtle break between the snow and rain areas seen previously, and corresponds reasonably well to the clearing observed on satellite imagery (Fig. 2b). A similar vertical motion profile was obtained for the cross-section 2° longitude to the west of the original cross-section, with slightly stronger values noted for the northern maximum (not shown). However, the pattern was less-defined for the cross-section 2° longitude to the east, as the southern maximum became more dominant. Once again, this pattern is consistent with the precipitation profile of Fig. 2a, indicating a reasonable forecast by the NGM.

By way of comparison, the 12-hour Eta forecast of vertical velocity did not portray the two separate areas of vertical motion. Instead, it was characterized by a continuous region of modest upward vertical motion spanning the snow and rain areas (Figs. 10a-b). Based on the observed precipitation pattern (Fig. 2a) and infrared satellite imagery (Fig. 2b), the vertical motion pattern of the NGM appeared more realistic. This will further be substantiated as we next examine the surface frontal-circulation.

The combination of lower-tropospheric frontogenesis and a thermally-direct transverse ageostrophic circulation appeared to help produce the strong vertical motion in the vicinity of the rain band. First, strong low-level convergence was evident at the front in the vicinity of 35 °N (Fig. 11). This convergence zone rapidly weakens along the deepening front to the north. This pattern is typical of many surface fronts as horizontal deformation is dominant in controlling surface frontogenesis (Keyser 1986). Utilizing (1), frontogenesis was noted at 1000 mb from eastern Colorado and New Mexico to northern Michigan (Fig. 12). There is a very good correspondence between the observed surface front and precipitation (Fig. 2a) and the

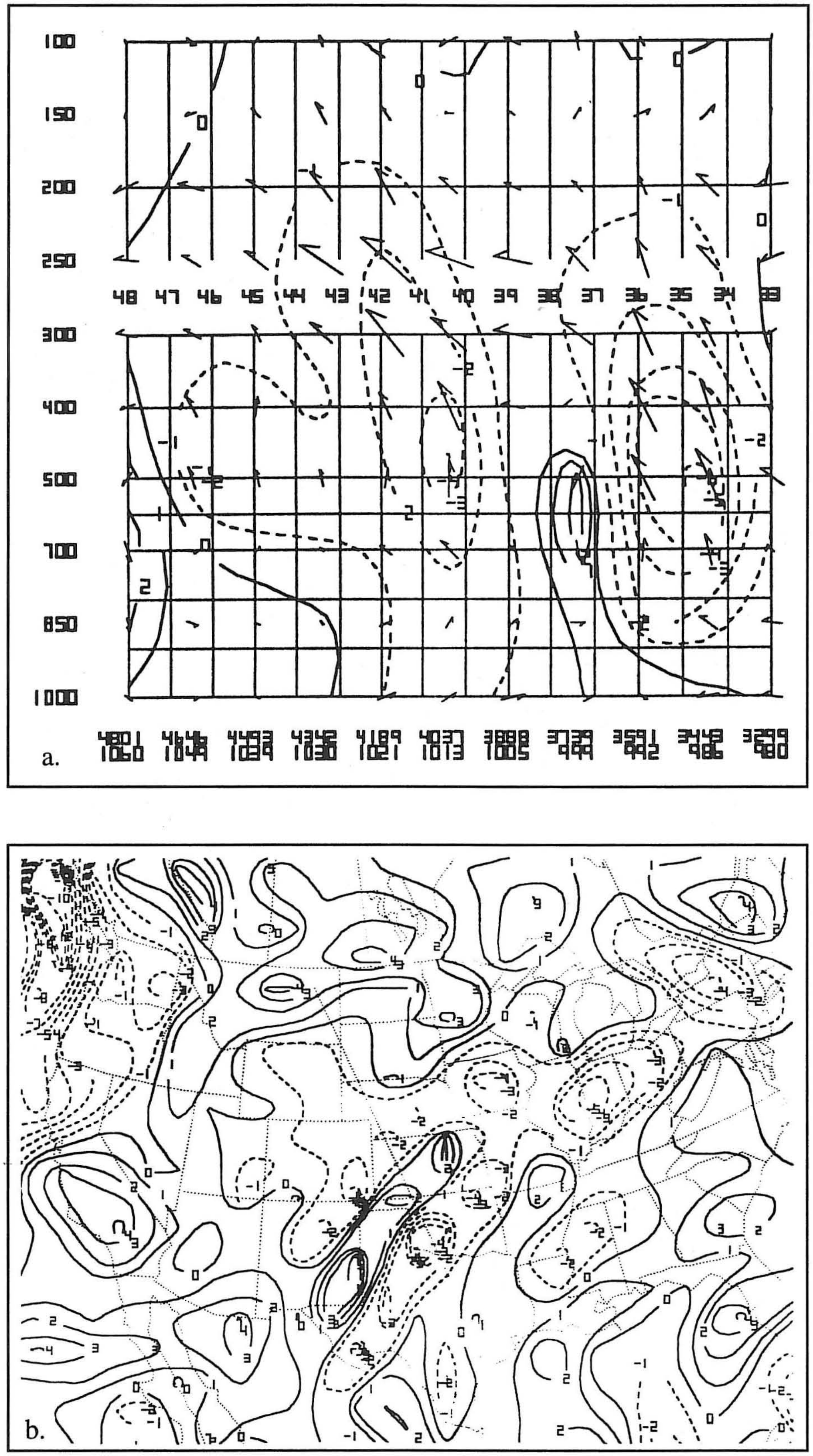

Fig. 9. (a) The 12-hour NGM forecast cross-section of the tangential ageostrophic wind (arrows), and the vertical velocity (dashed negative, 1 μbar s^{-1} intervals) valid 0000 UTC 9 November 1994. Vertical magnitude of arrows proportional to vertical velocity. Cross-section same as Fig. 6. (b) The 12-hour NGM forecast of the 700-mb vertical velocity (dashed negative, 1 μbar s^{-1} intervals) valid 0000 UTC 9 November 1994. Dashed values indicate upward vertical motion. The thin dotted line is the same as in Fig. 1.

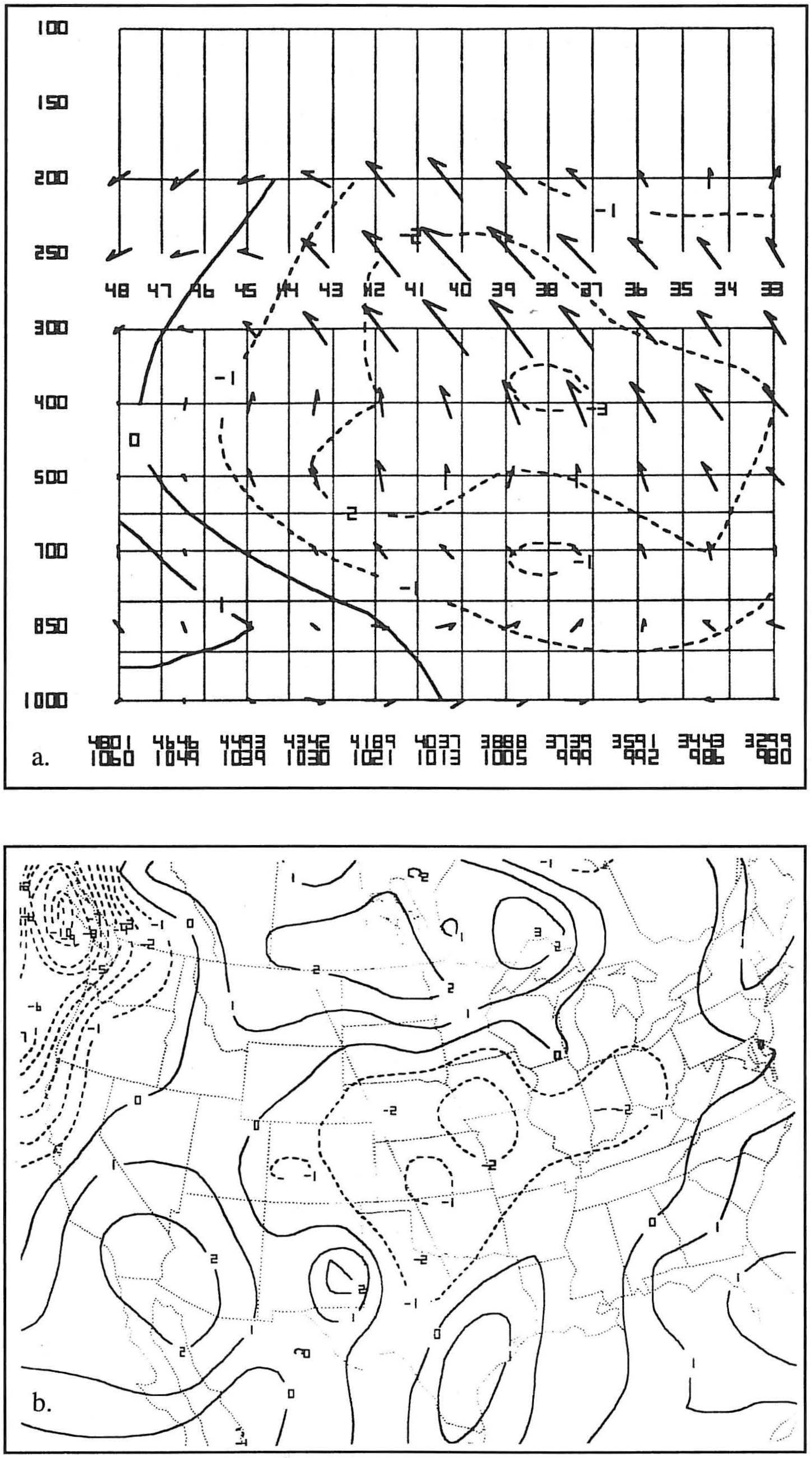

Fig. 10. Same as Fig. 9 except for the 12-hour Eta forecast.

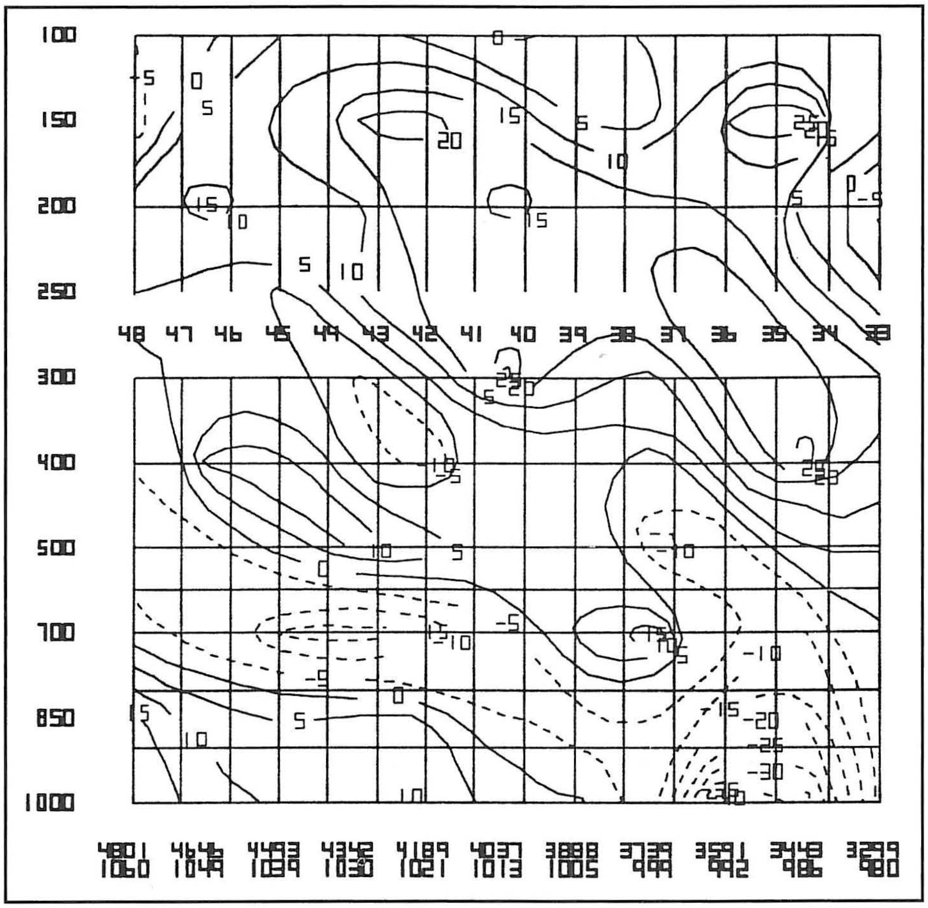

Fig. 11. The 12-hour NGM forecast cross-section of the divergence of the ageostrophic wind (dashed negative, 5 × 10^{-6} s^{-1} intervals) valid 0000 UTC 9 November 1994. Negative values denote convergence. Cross-section same as Fig. 6.

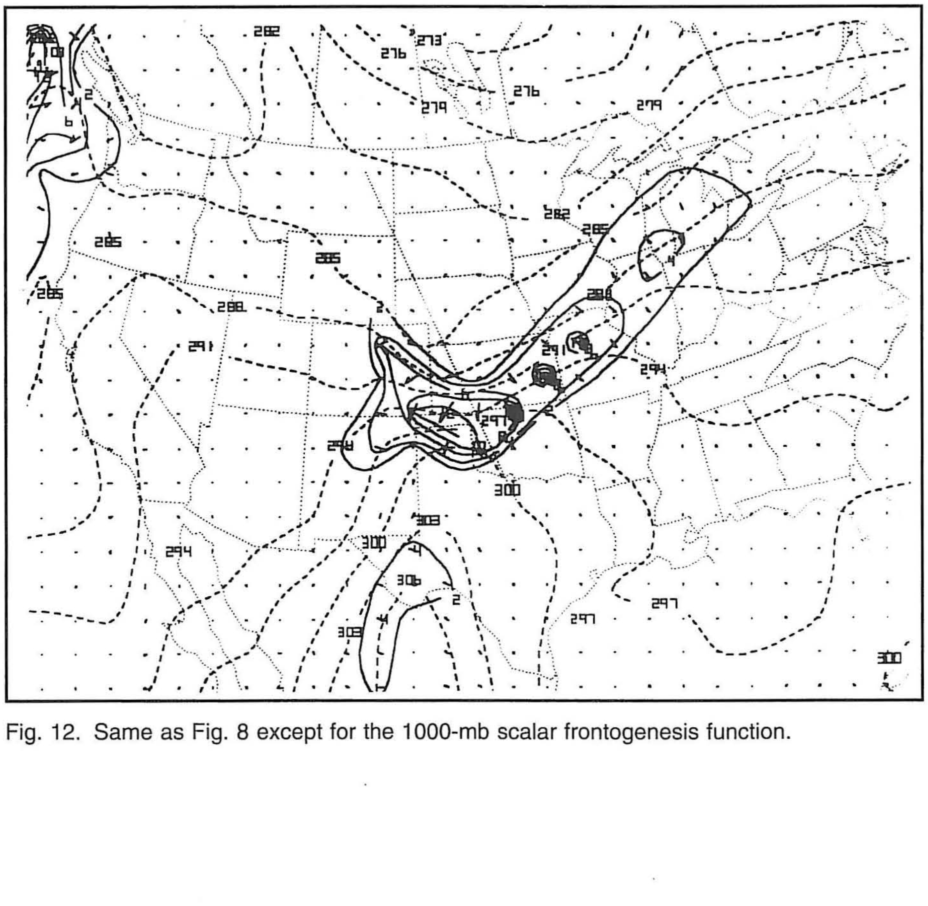

Fig. 12. Same as Fig. 8 except for the 1000-mb scalar frontogenesis function.

forecast 1000-mb frontogenesis (Fig. 12). [Albeit, the pattern was displaced slightly too far south as was the vertical motion field.] Since frontogenesis strengthens the local temperature gradient and tends to destroy the thermal wind balance, a thermally-direct transverse ageostrophic circulation necessarily develops normal to the front (Sawyer 1956). The ψ-vector (2) represents the lower branch of this ageostrophic flow, and points from cold to warm air in the case of frontogenesis, similar to the Q-vector (Sanders and Hoskins 1990; Augustine and Caracena 1994). Thus, sinking motion on the cold side of the front adiabatically warms and rising motion on the warm side of the front adiabatically cools; this tends to weaken the horizontal temperature gradient, thereby restoring thermal wind balance. Note how the ψ-vectors point from lower potential temperature to higher potential temperature in proximity to the frontogenesis (Fig. 12), implying the presence of a thermally-direct transverse ageostrophic circulation.

Referring again to Figure 9a (which is a cross-section of the PC-GRIDDS-derived ageostrophic wind-field), a thermally-direct transverse ageostrophic circulation was present in the vicinity of the frontal zone. The ageostrophic flow was directed from cold air to warm air in the lower troposphere (around 37 °N), consistent with the ψ-vectors in Fig. 12. The ascent branch of the circulation was near 34.5 °N and the descent branch of the circulation was near 37.5 °N (Fig. 9a), which straddled the surface frontal zone. This further suggests that the frontogenesis provided some of the forcing required for the upward vertical motion and observed precipitation. Based on the above discussion, the NGM vertical motion field was superior to that of the Eta since it was able to resolve this circulation, and gives impetus for trying to understand the causes of the model vertical motion field as mentioned in the Introduction. Of additional interest, the low-level convergence associated with the surface front was coupled with divergence in the 450-100 mb layer (Fig. 11), implying upward vertical motion according to the continuity equation (Holton 1992). These processes would not have been directly observable using conventional operational forecasting mechanisms.

Finally, modest lower-tropospheric warm air advection (WAA) was also present near the surface cold front (Fig. 13). The pattern of WAA between 1000 and 850 mb (Fig. 13b) was very similar to that of the 1000-mb frontogenesis (Fig. 12), but it was shifted slightly to the south. This WAA was likely augmenting the frontal circulation by supplying additional lift and destabilization. Viewed in terms of an isentropic framework, the WAA was providing only modest lift (not shown). In addition, Q-vector convergence (as is discussed later) was negligible from Texas to Michigan, further indicating that the WAA was ancillary in terms of vertical motion forcing.

Some insight into the forcing for the second area of vertical motion can be gleaned from looking at a cross-section of the advection of vorticity by the total wind along the cross-section shown earlier (Fig. 14a). In this illustration, one quickly observes a maximum between 44° N and 40° N at the 250-mb level. [This was associated with the cyclonic vorticity maximum noted in Fig. 7b.] According to quasi-geostrophic theory, rising motion is proportional to the rate of increase with height of CVA, plus positive thickness (warm air) advection (Holton 1992, pp. 166–170). Increasing CVA with height implies a falling geopotential, and adiabatic cooling through rising motion is one way the atmosphere can adjust to maintain a hydrostatic temperature field. Increasing CVA with height was noted between 500 mb and 250 mb over the area receiving snow (Figs. 2a and 14a), with relatively little difference in CVA with height prevalent in conjunction with the rain band. The observed pattern (Fig. 14a) suggests that upward vertical motion attending the snow band was forced (at least in part) by this increasing CVA with height. It is also interesting to note that vorticity advection was near zero at the 500-mb level; which, when again viewed on a traditional 500-mb forecast chart, may erroneously have led the forecaster to believe that there was little dynamical forcing owing to this factor. [Maximum CVA at 500 mb was actually forecast in southern New Mexico!]

Another desirable feature of PC-GRIDDS is the ability to compute layer differences, which helps to provide further confirmation of the dynamical link to the upward vertical motion and snowfall over Colorado and Nebraska. Using the 500-250 mb layer (based on Fig. 14a), increasing CVA with height was associated with nearly all of the Colorado and Nebraska precipitation (Fig. 14b). The change of CVA with height was insignificant in this layer for the precipitation noted along the surface front, and decreasing CVA with height was concomitant with the precipitation that occurred across the southern Great Lakes region (Fig. 14b). The patterns of vertical velocity (Fig. 9b) and increasing CVA with height (Fig. 14b) also correspond well with the left exit region of the cyclonically-curved jet-streak discussed earlier. The above results support the notion that increasing CVA with height (possibly forced by the jet-streak over New Mexico) was a significant factor in aiding the upward vertical motion and precipitation over Colorado and Nebraska. Furthermore, it is evident that CVA had little dynamical link to the precipitation along the surface front, as was discussed earlier.

To view the total quasi-geostrophic forcing, one should take into account both terms of the quasi-geostrophic omega equation (i.e., CVA and temperature advection). Perhaps the best and most widely used approach for this task is application of the Q-vector (Durran and Snellman 1987). Replacing the actual wind with the geostrophic wind in (2), and multiplying each component by R/p, one obtains the formulation of the Q-vector. Upward vertical motion is implied where the Q-vectors converge. Using the modification of (2), Q-vector convergence for the 500-250 mb layer was prevalent in an area similar to that of the increasing CVA with height (Fig. 15a), including the area of precipitation from Colorado to southeastern South Dakota. In the 850-500 mb layer, Q-vector convergence was noted primarily in eastern Colorado (Fig. 15b), which was influenced more strongly by WAA than at the upper-levels (not shown). Quasi-geostrophic forcing was not apparent in association with the rain band as Q-vector convergence was negligible in this area. Using the preceding approach, one could now apply scientific reasoning to why the snow fell in the vicinity of a surface high pressure (i.e., quasi-geostrophic forcing was prevalent), and hopefully would have lent itself to a more accurate and confident forecast.

In addition to the quasi-geostrophic forcing attending the snow band, orographically-induced uplift was evident across northeastern Colorado and western Nebraska. The inferred surface wind flow was from the northeast across this region (Fig. 2a), and this provided a component of upslope flow. The 12-hour forecast of the 1000-850 mb mean wind and vertical velocity (not shown) provides further support of this occurrence. Although the upslope flow may have contributed to the precipitation and upward vertical motion in the lower parts of the troposphere, the upper-level forcing was dominant (Fig. 9a) and is believed to be the primary cause of the snow band. Nevertheless, the synergism of these two factors (possibly through the seeder-feeder process) to perhaps enhance the snowfall was clearly observable via evaluation with PC-

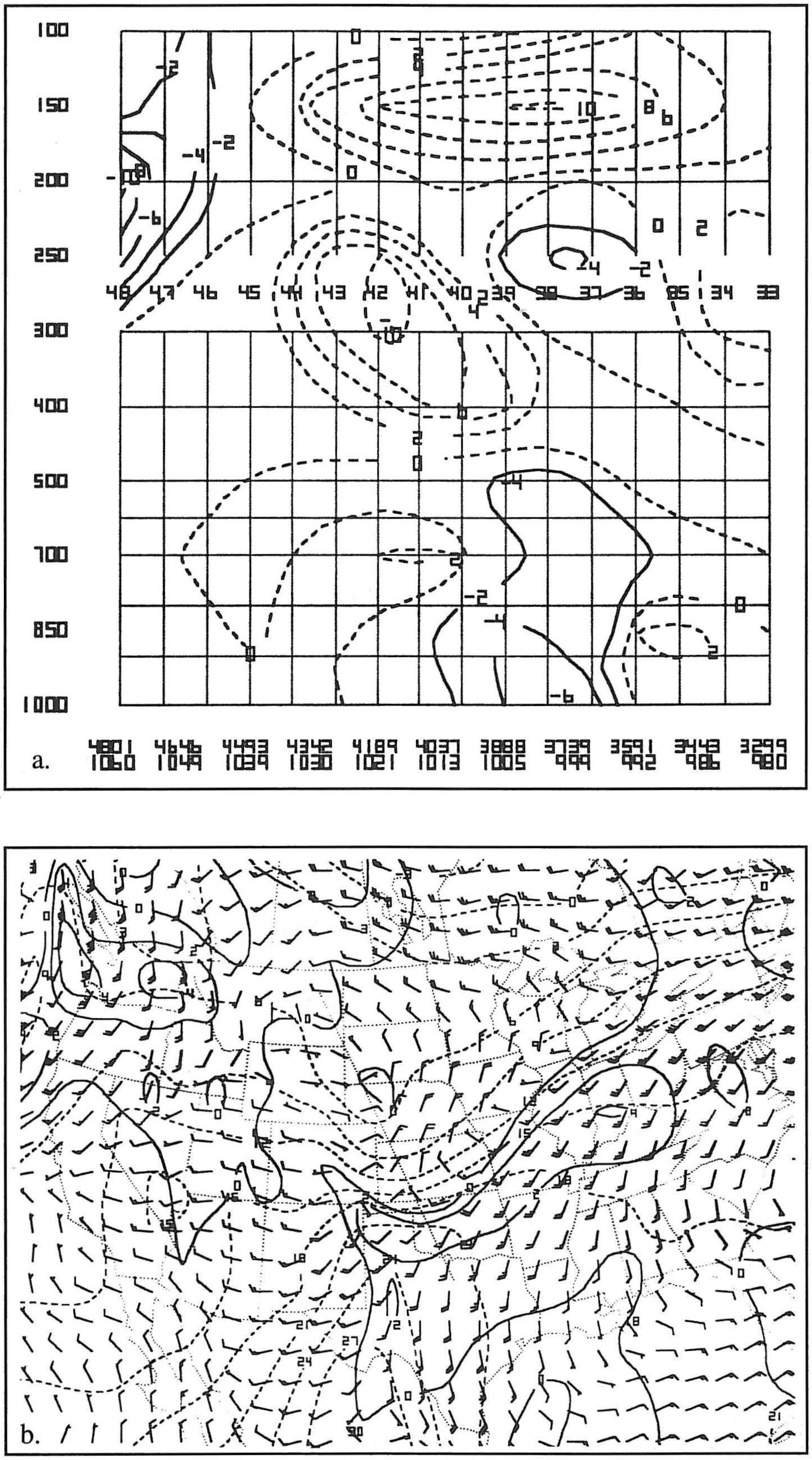

Fig. 13. (a) The 12-hour NGM forecast cross-section of the hourly temperature advection by the total wind (dashed positive, 2×10^{-1} K hr^{-1} intervals) valid 0000 UTC 9 November 1994. Cross-section same as Fig. 6. (b) The 12-hour NGM forecast of the 1000-850 mb layer: warm air advection (solid, 2×10^{-1} K hr^{-1} intervals), temperature (dashed, 3 °C intervals), and wind (kt) valid 0000 UTC 9 November 1994. The thin dotted line is the same as in Fig. 1.

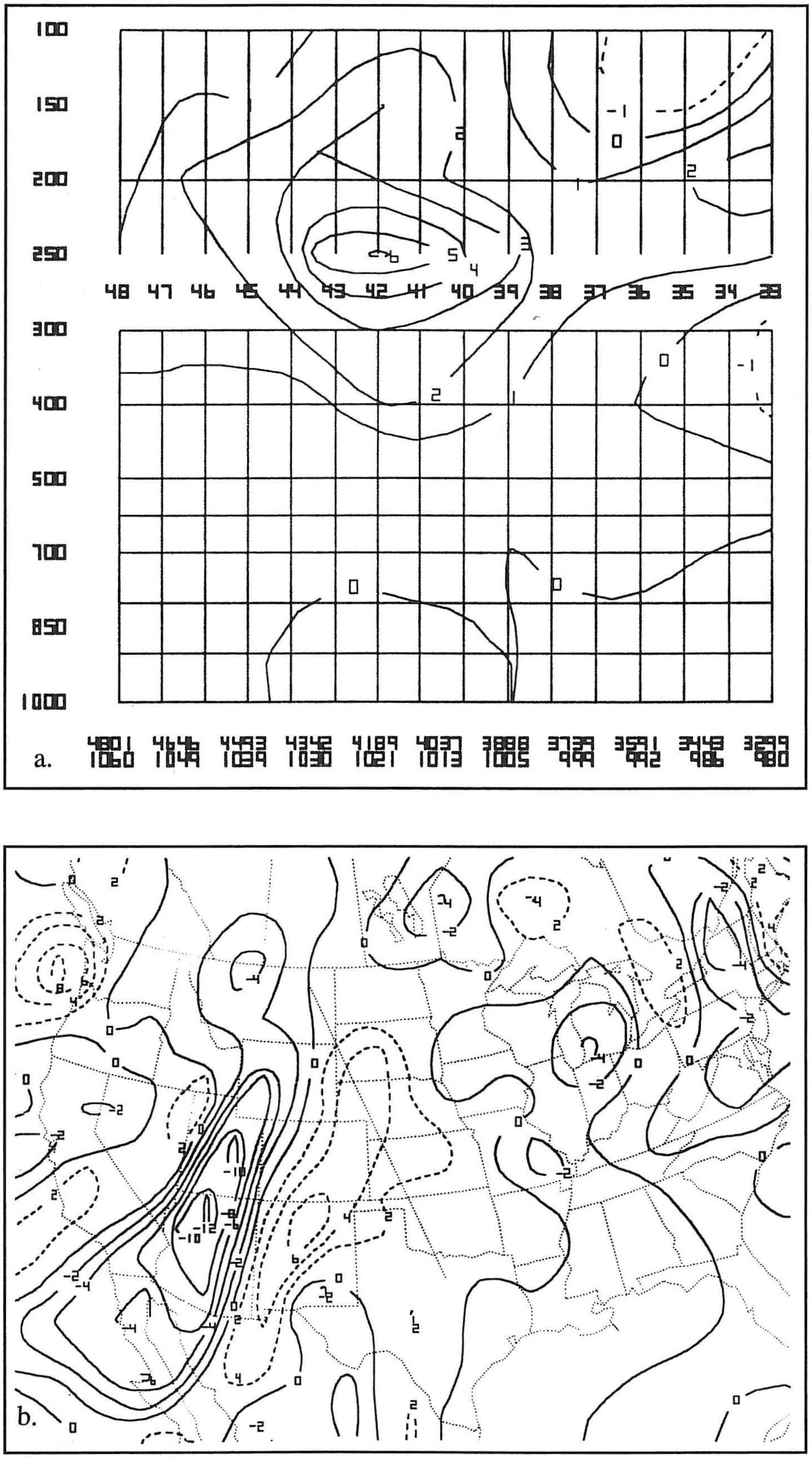

Fig. 14. (a) The 12-hour NGM forecast cross-section of the vorticity advection by the total wind (dashed negative, 1×10^{-9} m s^{-2} intervals) valid 0000 UTC 9 November 1994. Cross-section same as Fig. 6. (b) The 12-hour NGM forecast of the 500-250 mb layer difference in vorticity advection (dashed positive, 2×10^{-9} m s^{-2} intervals) valid 0000 UTC 9 November 1994. Positive values denote increasing cyclonic vorticity advection with height. The thin dotted line is the same as in Fig. 1.

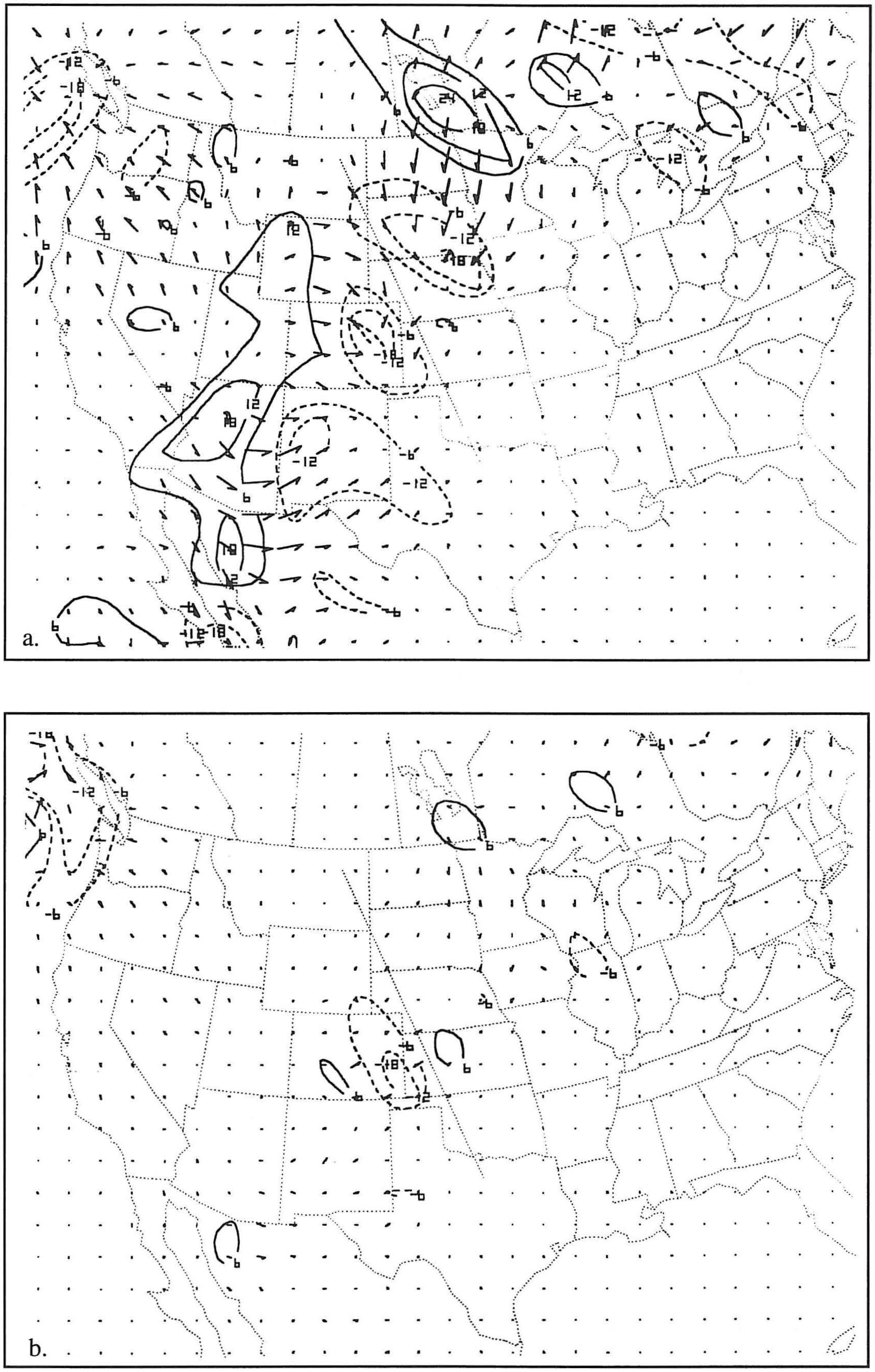

Fig. 15. The 12-hour NGM forecast of: (a) the 500-250 mb Q-vectors and Q-vector convergence (dashed negative, 6 × 10^{-19} m kg^{-1} s^{-1} intervals), and (b) the 850-500 mb Q-vectors and Q-vector convergence (dashed negative, 6 × 10^{-19} m kg^{-1} s^{-1} intervals) valid 0000 UTC 9 November 1994. Negative values denote convergence. The thin dotted line is the same as in Fig. 1.

GRIDDS, and lends credence to operational forecasting utilizing gridded model data.

Finally, the two regions of upward vertical motion (both model-derived and estimated) were not entirely associated with precipitation. It is understood that adequate moisture is also essential for precipitation formation, and that when combined with the vertical motion field, clouds and precipitation can be more reliably inferred. However, the intent of this case-study was only to show how gridded model data can be used to investigate the processes related to the upward vertical motion and their association with the precipitation. In the operational setting, moisture availability and atmospheric stability also need to be addressed. For this case, the 12-hour NGM forecast of the surface to 500 mb relative humidity indicated available moisture for the region of snowfall (> 70%), with only moderate moisture (50%) along the surface front (not shown). Other factors, such as stability and low-level moisture, would have also been important when assessing the potential for precipitation along the front.

4. Summary

An extratropical storm on 8 November 1994 was examined via PC-GRIDDS where an area of snow was occurring near a surface anticyclone, and a rain band was associated with a surface frontal zone. The 12-hour NGM forecast reasonably predicted the synoptic pattern attending the storm, and, in addition, an upper-level front and tropopause fold were indicated (despite the relatively poor vertical resolution offered by PC-GRIDDS). Although a jet-streak over the Great Lakes was accurately forecast, another 300-mb jet-streak that was entering the southwestern United States went underforecast at 12 hours, and such an occurrence has been previously documented (Barnes and Colman 1994). Increasing CVA with height and modest WAA (Q-vector convergence), played an integral role in developing the region of upward vertical motion that sustained the widespread area of light to moderate snow, consistent with quasi-geostrophic theory (Holton 1992). This may have been associated with the left exit region of the jet-streak over New Mexico, but is difficult to tell from the 12-hour forecast since this jet was underforecast. In contrast, the frontal precipitation was aided by the synergism of low-level frontogenesis, its attendant thermally-direct transverse ageostrophic circulation, and modest lower-tropospheric WAA. Using this process of estimating the vertical motion field, and comparing it to the model derived field, the 12-hour NGM forecast (Fig. 9) was preferred to that of the Eta (Fig. 10). As a final note, the 00-hour NGM forecast from 0000 UTC 9 November 1994 maintained the two distinct areas of upward vertical motion, as well as the thermally-direct lower-tropospheric frontal circulation.

This case illustrates that PC-GRIDDS can be an effective tool in analyzing areas of upward vertical motion associated with various dynamical processes. In a situation where conventional forecast tools may have been misleading (e.g., Labas 1994), use of PC-GRIDDS was able to reveal the physical processes at work and provide a solid scientific understanding of their origin (as well as help determine which model vertical velocity field was more representative). Although the NGM produced a reasonable forecast of the vertical motion patterns and tropospheric features, one must continually be aware of how the models are performing. Before one can effectively use PC-GRIDDS, an understanding of the synoptic setting and the verity of the latest NCEP model runs needs to be ascertained. In addition, in order to glean the full benefits of PC-GRIDDS (or any other software program capable of dissecting model gridded data), it is desirable to have a comprehensive background of meteorological process and conceptual models that help to explain sensible weather.

Acknowledgments

The author would like to thank Brian Klimowski and Don Reed at the National Weather Service office in Rapid City; Norman Junker at the National Centers for Environmental Prediction; Ed Berry and Preston Leftwich at the National Weather Service Central Region Scientific Services Division; and *National Weather Digest* co-editor Richard McNulty for their insightful reviewing comments. Figure 3b was provided by the Institute of Atmospheric Sciences at the South Dakota School of Mines & Technology.

Author

Matthew Bunkers became a Meteorologist in October of 1995 at the National Weather Service (NWS) office in Rapid City, South Dakota. Initially, Matt joined the NWS in June of 1991 as part of a cooperative agreement with the South Dakota School of Mines and Technology (SDSM&T) in Rapid City. He worked part-time until December of 1993, when he became a Meteorologist Intern. Matt earned both his B.S. Degree in Interdisciplinary Sciences (May 1992) and his M.S. Degree in Meteorology (December 1993) from SDSM&T. His interests vary widely among El Niño/La Niña, winter storms, severe convection, flash flooding, and climatology. In addition to co-authoring a NWS Central Region Technical Attachment pertaining to a Black Hill's landspout, Matthew has co-authored two articles on cluster analysis and El Niño/La Niña for the *Journal of Climate*.

References

Augustine, J. A., and F. Caracena, 1994: Lower-tropospheric precursors to nocturnal MCS development over the central United States. *Wea. Forecasting*, 9, 116–135.

Barnes, S. L., and B. R. Colman, 1994: Diagnosing an operational numerical model using Q-vector and potential vorticity concepts. *Wea. Forecasting*, 9, 85–102.

Dunn, L. B., 1991: Evaluation of vertical motion: Past, present, and future. *Wea. Forecasting*, 6, 65–75.

Durran, D. R., and L. W. Snellman, 1987: The diagnosis of synoptic-scale vertical motion in an operational environment. *Wea. Forecasting*, 2, 17–31.

Hakim, G. J., and L. W. Uccellini, 1992: Diagnosing coupled jet-streak circulations for a Northern Plains snow band from the operational nested-grid model. *Wea. Forecasting*, 7, 26–48.

Holton, J. R., 1992: *An Introduction to Dynamic Meteorology*. Academic Press, San Diego, 507 pp.

Keyser, D., 1986: Atmospheric fronts: An observational perspective. *Mesoscale Meteorology and Forecasting*, P. S. Ray, Ed., Amer. Meteor. Soc., Boston, 216–258.

_______________, M. J. Reeder, and R. J. Reed, 1988: A generalization of Petterssen's frontogenesis function and its relation to the forcing of vertical motion. *Mon. Wea. Rev.*, 116, 762–780.

Labas, K. M., 1994: Views of vertical motion associated with a jet streak through the eyes of PCGRIDDS. National Weather Service, Central Region Tech. Attach. 94–10, 8 pp.

Meier, K. W., 1993: *PC-GRIDDS User's Manual*: Ver. 12/93. National Weather Service, Western Region, Scientific Services Division, 102 pp.

Moore, J. T., and G. E. VanKnowe, 1992: The effect of jet-streak curvature on kinematic fields. *Mon. Wea. Rev.*, 120, 2429–2441.

Noah, D. G., 1994: Application of the dual jet-streak conceptual model via PCGRIDDS. National Weather Service, Central Region Tech. Attach. 94-16, 9 pp.

Petersen, R. A., 1992: A PC-based system for the display of gridded WAFS data. *Proceedings of the WMO Technical Conference on Tropical Aeronautical Meteorology* (TECTAM-92), Geneva, Switzerland.

Sanders, F., and B. J. Hoskins, 1990: An easy method for estimation of Q-vectors from weather maps. *Wea. Forecasting*, 5, 346–353.

Sawyer, J. S., 1956: The vertical circulation at meteorological fronts and its relation to frontogenesis. *Proc. Roy. Soc. London*, A234, 346–362.

Shapiro, M. A., 1981: Frontogenesis and geostrophically forced secondary circulations in the vicinity of jet stream-frontal zone systems. *J. Atmos. Sci.*, 38, 954–973.

____________, and D. Keyser, 1990: Fronts, jet streams and the tropopause. *Extratropical Cyclones: The Erik Palmén Memorial Volume*. C. W. Newton and E. O. Holopainen, Eds., Amer. Meteor. Soc., Boston, 167–191.

Uccellini, L. W., and P. J. Kocin, 1987: The interaction of jet streak circulations during heavy snow events along the east coast of the United States. *Wea. Forecasting*, 2, 289–308.

____________, 1990: The relationship between jet streaks and severe convective storm systems. *Preprints, 16th Conf. on Severe Local Storms*, Kananaskis Park, Alberta, Canada, Amer. Meteor. Soc., 121–130.